CH9800023

Simulations of Ion-Temperature-Gradient modes in helical symmetry

L. Villard, M. Fivaz, J. Vaclavik
Centre de Recherches en Physique des Plasmas, Association Euratom - Confédération Suisse, Ecole Polytechnique Fédérale de Lausanne

Abstract. We present the first simulations of Ion Temperature Gradient (ITG) modes in straight helical configurations. A linear particle-in-cell gyrokinetic global code initially developed for toroidal axisymmetric geometry [1, 2] has been modified to treat the case of helical symmetry. The model is based on gyrokinetic ions, adiabatic electrons and electrostatic quasineutral perturbations. The code simulates the full plasma cross-section. The potential is represented on a magnetic coordinate system and discretized with finite elements. Analytical extraction of the fast poloidal variation is done on a straight field line coordinate, allowing a speedup of one or two orders of magnitude. A $l = 1$ vacuum field configurations is studied. The very low shear and small ∇B drifts imply that for a wide range of parameters the most unstable ITG modes are "slab-like".

Introduction. Anomalous transport in magnetically confined plasmas is widely believed to be attributed to micro-instabilities of low frequency drift-wave type. Over the past years the efforts in the theoretical analysis have focused on axisymmetric configurations of the tokamak type. In contrast, very little has been done for stellarators: previous works on drift waves [3] - [6] have so far been limited to simple cold ion electrostatic models with local and ballooning approximations. The present work is the first that addresses the question of Ion-Temperature-Gradient (ITG) modes in helical geometry. The specific objective is to get an understanding of ITG modes and to compare with the tokamak results. The longer term goal is to understand whether or not transport in stellarators, if determined by such micro-instabilities, can be different from that in a tokamak.

Helical Geometry. In this paper we shall consider helical symmetry (i.e. straight stellarators). Let r, φ, z be the cylindrical coordinates. Helical symmetry implies that all scalar equilibrium fields can be expressed as functions of two variables: r and $\zeta = \varphi - hz$, where h is the helicity. A toroidal configuration of N_{per} field periods and major radius R_0 is thus modeled by a helicity $h = N_{per}/R_0$. Let us introduce the following coordinates: a helical system (x', y') with $x' = r\cos\zeta$, $y' = r\sin\zeta$, and a magnetic coordinate system (s, θ) with $s = ((\psi - \psi_{min})/(\psi_{max} - \psi_{min}))^{1/2}$, where ψ is the helical flux, $\theta = \arctan(y'/(x' - x'_m))$, where the magnetic axis position is $(x' = x'_m, y' = 0)$. In addition to the "poloidal" coordinate θ, we introduce the straight field line coordinate χ

$$\tilde{q} = \frac{h}{2\pi}\int_0^{2\pi} \frac{\mathbf{B}\cdot\nabla z}{\mathbf{B}\cdot\nabla\theta} d\theta \qquad \chi = \frac{h}{\tilde{q}}\int_0^{\theta} \frac{\mathbf{B}\cdot\nabla z}{\mathbf{B}\cdot\nabla\theta} d\theta \tag{1}$$

where the integrals are on a $\psi = const$ surface. Note that with this definition the rotational transform per helical period length $L = 2\pi/h$ is $\iota = 1/\tilde{q} + 1$.

The equilibrium magnetic field is given by the representation

$$\mathbf{B} = F\mathbf{u} + \nabla\psi \times \mathbf{u} \qquad \mathbf{u} = (hr\mathbf{e}_\varphi + \mathbf{e}_z)/(1 + h^2r^2) \tag{2}$$

with F a function of ψ so that $\mathbf{B}$ satisfies the helical symmetry and $\nabla\cdot\mathbf{B} = 0$. In this

paper we shall restrict ourselves to vacuum fields. They can be expressed as

$$\psi = \frac{1}{2}Fhr^2 - r\sum_l b_l I_l'(lhr)\cos(l\zeta) \tag{3}$$

where F is a constant and I_l is the modified Bessel function of order l.

Gyrokinetic model. The plasma ions are described with a linearized gyrokinetic model with the usual ordering: $\omega/\Omega \sim k_\parallel/k_\perp \sim e\phi/T_e \sim \rho/L_n \sim \rho/L_T \sim \mathcal{O}(\epsilon_g)$, where ρ is the ion Larmor radius, Ω is the ion cyclotron frequency, $L_E^{-1} = |\nabla \ln E|, E = n_0, T$. Another small parameter is $\rho/L_B \sim \mathcal{O}(\epsilon_B)$, with $L_B = B/|\nabla B|$. Consistent with the gyrokinetic ordering, the perturbations of interest have $k_\parallel << k_\perp$. We use this property to extract the poloidal phase variation of the mode

$$f(\mathbf{x},t) = \tilde{f}(s,\theta,t)e^{iS} \qquad \phi(\mathbf{x},t) = \tilde{\phi}(s,\theta,t)e^{iS} \qquad S(s,\theta,z) = m_0\chi(s_0,\theta) + kz - \omega_0 t \tag{4}$$

where $k = hn/N_{per}$, n is the "helical" mode number, the magnetic surface $s = s_0$ is chosen near the expected maximum mode amplitude, m_0 is an integer close to $-n\tilde{q}_0/N_{per}$, and $\tilde{q}_0 = \tilde{q}(s_0)$. Note that a perturbation having a single Fourier component m in the straight field line poloidal angle χ has

$$k_{\parallel,m} = \frac{B_z}{B}h(\frac{m}{\tilde{q}} + \frac{n}{N_{per}}). \tag{5}$$

The transformed quantities $(\tilde{\phi}, \tilde{f})$ are expected to have a slow poloidal variation, the fast variation having been extracted by the phase factor. This technique will allow us to study high n modes with the same computational performance as low n modes. The quantity ω_0 is not the eigenfrequency but serves to shift the simulated frequencies; this is particularly useful to study modes near the marginal stability with $\gamma << \omega$.

The unperturbed trajectories of the guiding centres (GC) have three constants of motion: the kinetic energy, the magnetic moment and the helical canonical momentum $\Psi_0 = \psi + (m_i/q_i)v_\parallel F/B$. The equilibrium ion distribution function f_0 is assumed isotropic Maxwellian with density and temperature constant on a magnetic surface. The perturbed distribution function is evolved along the unperturbed trajectories. The electrons are assumed to respond adiabatically. The quasi-neutrality condition, in which the polarization density is approximated by a differential expression valid up to $(k_\perp\rho)^2$, close the system of equations:

$$\frac{d\mathbf{R}}{dt} = v_\parallel \mathbf{e}_\parallel + \frac{v_\parallel^2 + v_\perp^2/2}{\Omega}\mathbf{e}_\parallel \times \nabla \ln B, \quad \frac{dv_\parallel}{dt} = \frac{1}{2}v_\perp^2 \nabla\cdot\mathbf{e}_\parallel, \quad \frac{dv_\perp}{dt} = -\frac{1}{2}v_\perp v_\parallel \nabla\cdot\mathbf{e}_\parallel \tag{6}$$

$$\frac{d\tilde{f}}{dt} + i\frac{dS}{dt}\tilde{f} = \frac{-\tilde{\mathbf{E}}}{B}\cdot\left((\mathbf{e}_\parallel \times \nabla\psi)\frac{\partial f_0}{\partial \psi} + \Omega\mathbf{e}_\parallel\frac{\partial f_0}{\partial v_\parallel} + (\mathbf{e}_\parallel \times \nabla \ln B)\left(v_\parallel\frac{\partial f_0}{\partial v_\parallel} + \frac{1}{2}v_\perp\frac{\partial f_0}{\partial v_\perp}\right)\right) \tag{7}$$

$$\tilde{\mathbf{E}}(\mathbf{R}, v_\perp) = -\frac{1}{2\pi}\int \mathcal{G}\tilde{\phi}(\mathbf{x})\delta(\mathbf{x} - \mathbf{R} + \boldsymbol{\rho})e^{i(S(\mathbf{x}) - S(\mathbf{R}))}d\mathbf{x}d\alpha \tag{8}$$

$$\frac{n_0 e}{T_e}\tilde{\phi}(\mathbf{x}) - \mathcal{G}_\perp\cdot\frac{n_0}{B\Omega}\mathcal{G}_\perp\tilde{\phi}(\mathbf{x}) = \int \tilde{f}(\mathbf{R}, v_\parallel, v_\perp)\delta(\mathbf{R} - \mathbf{x} + \boldsymbol{\rho})e^{i(S(\mathbf{R}) - S(\mathbf{x}))}d\mathbf{R}d\mathbf{v} \tag{9}$$

where $\mathcal{G} = (i\nabla S + \nabla)$.

The distribution function $\tilde{f}$ is discretized in a 4-D reduced phase space $(x', y', v_{||}, v_{\perp})$. The potential $\tilde{\phi}$ is discretized with quadratic spline finite elements in (s, θ). The new version of the code has been benchmarked against the axisymmetric version by considering a straight field configuration ($T = B_0 = const, b_l = 0$). We have checked that the results coincide and are independent of the helicity h. Convergence with the timestep, the mesh and the number of particles, and power consistency have been demonstrated.

Results. We consider the following $l = 1$ configuration: $F = 1T$, $b_1 = 0.5T$, $a = 0.5m$, $h = 1m^{-1}$, flat density, $T_e = T_i$, $d\ln T_i/ds$ profile peaking at $s = s_0 = 0.5$ with $L_T/a = 0.1$, $T_i(s_0) = 4keV$. This configuration has a flat $\tilde{q}$ profile: $\tilde{q}_{axis} = -1.0405$, $\tilde{q}_{edge} = -1.0464$, implying that $k_{||,m}(s) \simeq const$. The magnetic gradients are rather small: $L_B/a \sim 8$ (therefore comparable to those of a tokamak of aspect ratio 8).

Simulations have been performed for various helical mode numbers n. The real frequencies ω and the growth rates γ are shown in Fig.1,left. For low n, both ω and γ increase linearly with n. A plot of the mode structure (Fig.1,right) shows a rather pure m poloidal dependence. For $n \geq 2$, $\omega > \omega_b$ and we do not expect to be in the trapped ion regime: this has been checked by artificially suppressing the $v_{||}$ and $v_{\perp}$ variation in Eq.(7) and the result is unchanged. Even for $n < 2$ we could not find a trapped ion mode, probably because of the small trapped particle fraction ($\simeq 0.25$). Therefore, for $n \leq 12$ the mode is a slab-ITG. As n is further increased, the mode structure becomes more complicated. In fact, in many cases, several modes are present in the simulation, indicating that two (or more) modes have similar γ but different ω. The interpretation of the PIC simulation results is therefore more difficult. In some cases we were able, by initializing different perturbations and shifting the frequency, to identify two competing modes. Another characteristic of the high n modes is that as n increases the mode amplitude tends to become higher in the unfavourable ∇B region (low field side). An example is shown in Fig.2,left. This behaviour is similar to that of the toroidal ITG in tokamaks. Here we have a "helical-ITG", but the mode structure does not show such a broad m spectrum as in a standard tokamak: even at high n, we do not have overlapping of several m's having resonance surfaces in the gradient region: either the whole plasma is resonant (e.g. for $m = 25, n = 24$) or it is not, because of the flat $\tilde{q}$. Another effect comes into play at high n: finite Larmor radius. For $n = 28$ we have $k_{\perp}\rho \simeq 1$ at $s = s_0$. The large damping tends to suppress the mode, and this is the reason of the decrease of γ for high n. This FLR effect is also responsible for the change in the mode localization (Fig.2,right): at high n it peaks at $s \simeq 0.6$ where T_i is smaller, whereas at low n it peaks at $s \simeq 0.4$. Thus $k_{\theta}\rho$ is nearly constant at the maximum radial mode localization, therefore ω is also nearly constant for $n > 22$.

Conclusion. These first simulations of ITG modes in a helical configuration indicate that the modes potentially creating the highest transport are slab-ITGs at relatively low n. The small ∇B and the very low shear are typical for such straight stellarators: these seem to be favourable properties to minimize ITG-based transport.

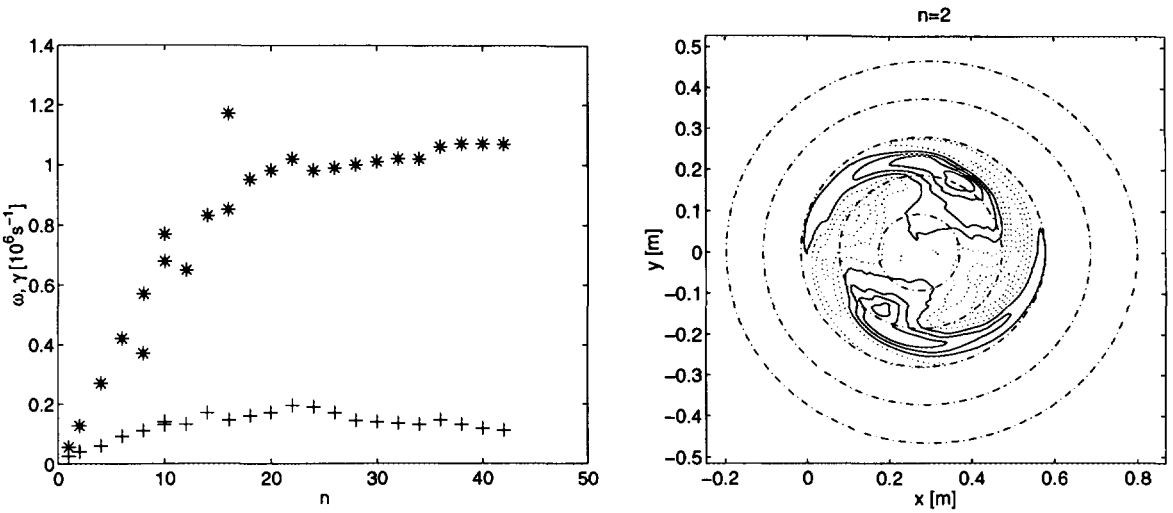

Figure 1: *Left: frequency ω (stars) and growth rate γ (crosses) as function of the helical mode number n. Right: contours of the perturbed potential ϕ for $n = 2$.*

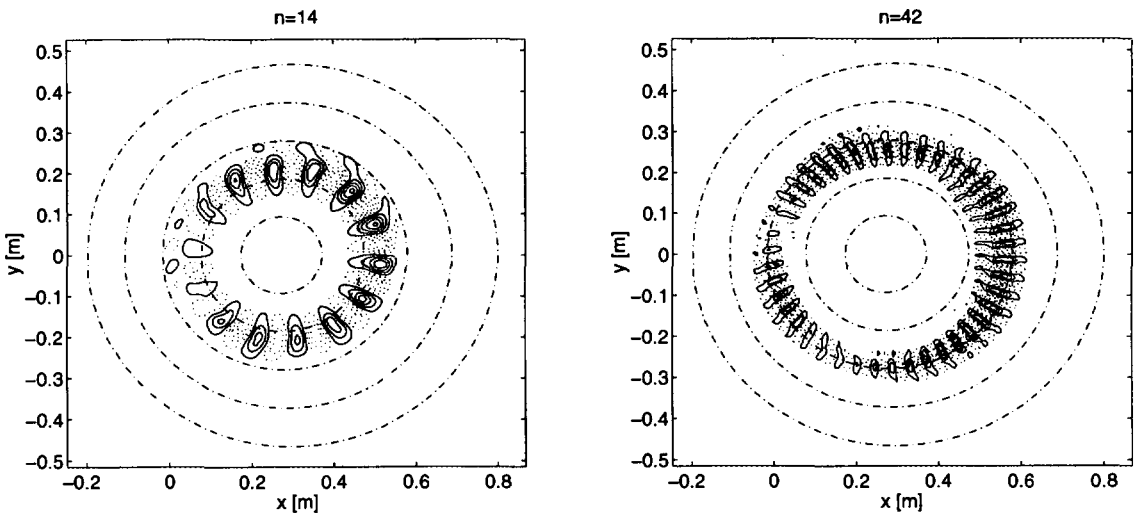

Figure 2: *Contours of the perturbed potential ϕ for $n = 14$ (left) and $n = 42$ (right) .*

Acknowledgements. This work was partly supported by the Swiss National Science Foundation. We thank W.A. Cooper and S. Brunner for helpful discussions.

References

[1] M. Fivaz, *et al.*, Theory of Fusion Plasmas, Int. Workshop, Varenna, August 1996, Editrice Compositori, Societa Italiana di Fisica, Bologna, 1997, p.485.

[2] M. Fivaz, Global ion-temperature-gradient instabilities in finite pressure tokamak plasmas, PhD Thesis no.1692(1997) EPFL, LRP 582/97.

[3] A. Bhattacharjee, *et al.*, Phys. Fluids 26 (1983) 880.

[4] N. Dominguez, *et al.*, (1992) 2894.

[5] R.E. Waltz, A.H. Boozer, Phys. Fluids B 5 (1993) 2201.

[6] M. Persson, J.L.V. Lewandowski, H. Nordman, Phys. Plasmas 3 (1996) 3720.